ChemPubSoc Europe

DOI: 10.1002/cctc.201200456

The Effect of the Fluorine Substitution on the Enantioselective Oxidation of Sulfides with Chiral Titanium Catalysts: A Combined Computational and Experimental Investigation

Maria Annunziata M. Capozzi,[b] Francesco Capitelli,[c] Andrea Bottoni,*[d] Matteo Calvaresi,[d] and Cosimo Cardellicchio*[a]

Dedicated to Prof. Francesco Naso on the occasion of his 75th birthday

The results of a combined computational-experimental study of the oxidation of various fluorinated aryl benzyl sulfides using *tert*-butyl hydroperoxide (TBHP) in the presence of a complex of titanium and (*S*,*S*)-hydrobenzoin are presented. As observed in previous studies for other aryl benzyl sulfides, the reaction leads to enantiopure sulfoxides (*ee* > 98%) in good isolated yields (81–96%) except the case of pentafluorobenzyl pentafluorophenyl sulfide for which a lower *ee* (61%) is observed. DFT computations on a model-system formed by the substrate, the oxidant TBHP and the [(*S*,*S*)-hydrobenzoin]$_2$-Ti complex satisfactorily explain this unexpected item. The enantioselectivity is governed by the relative energy of the two diastereomeric octahedral complexes that form if TBHP approaches the initial complex between substrate and [(*S*,*S*)-hydrobenzoin]$_2$-Ti before the oxygen transfer. For pentafluorobenzyl pentafluorophenyl sulfide, the two octahedral complexes are almost degenerate and, thus, they form in similar amounts. As the two corresponding diastereomeric transition states are similar in energy, the probability to follow one or the other diastereomeric reaction channel becomes comparable, which leads to the lower enantiomeric excess experimentally observed. Our computations indicate that the particular "folded conformation", adopted by the substrate only if both phenyl rings are fluorinated, is the key factor that determines the near degeneracy of the two diastereomeric octahedral complexes.

Introduction

Enantiopure sulfoxides are widely employed in stereoselective synthesis as useful chiral auxiliaries and intermediates; they can exert high asymmetric induction and are characterised by the significant configurational stability of the sulfinyl moiety.[1–4] In addition to their synthetic value, some chiral sulfoxides are of uttermost importance in medicinal chemistry and pharmacology thanks to their biological activity.[5–7] A notable example is the well-known anti-ulcer agent (*S*)-omeprazole,[6–7] which was sold for many years as a racemic mixture, but is now available on the market in enantiopure form.

Various methodologies have been proposed during the last half century for the synthesis of these valuable intermediates and a large number of examples are now available in literature[1–4] For instance, organometallic reagents can be used to displace leaving groups from suitable sulfinyl compounds with a complete inversion at the sulfur stereogenic centre.[1–3] The Andersen reaction, in which menthyl (*S*)- or (*R*)-*p*-toluenesulfinates react with Grignard reagents, can be considered the prototypical example of this procedure.[8,9]

An alternative methodology is the enantioselective oxidation of sulfides.[1–4] The most common catalysts of this type are based on titanium complexes, as proposed almost simultaneously and independently by Modena et al.[10] and Kagan et al.,[11] who used titanium *iso*-propoxide Ti(O-*i*Pr)$_4$ as a metal source, enantiopure diethyl tartrate as the chiral modifier and an alkyl hydroperoxide as the real oxidant. Since then, many different oxidation catalysts have been proposed,[1–4] and some of them have been successfully employed in the industrial productions of bioactive sulfoxides.[12]

In our previous work,[13–21] we have described the results obtained in the asymmetric synthesis of chiral non-racemic sulf-

[a] Dr. C. Cardellicchio
CNR ICCOM—Dipartimento di Chimica
Università di Bari
via Orabona 4. 70125 Bari (Italy)
Fax: (+39) 0805539596
E-mail: cardellicchio@ba.iccom.cnr.it

[b] Dr. M. A. M. Capozzi
Dipartimento di Chimica
Università di Bari
via Orabona 4. 70125 Bari (Italy)

[c] Dr. F. Capitelli
CNR IC
via Salaria, Km 29.300, 00195 Monterotondo (Rome)

[d] Prof. A. Bottoni, Dr. M. Calvaresi
Dipartimento di Chimica "G. Ciamician"
Università di Bologna
via Selmi 2, 40126 Bologna (Italy)

Supporting information for this article is available on the WWW under http://dx.doi.org/10.1002/cctc.201200456.

oxides using either enantioselective oxidation[15–21] or Grignard reagents reacting with suitable sulfinyl compounds.[13–17] In the latter case, unconventional displacement of carbanionic leaving groups was observed. However, during the last decade,[17–21] we have focused our research on the enantioselective oxidation of sulfides with hydroperoxides in the presence of catalytic amounts of a complex of titanium and (*S*,*S*)- or (*R*,*R*)-hydrobenzoin, which is a cheap and easily available chiral auxiliary.[22] This oxidation procedure is straightforward, because it proceeds at room temperature, non-chlorinated solvents are used and no particular experimental work-up is required. The use of a catalyst based on a metal complex of the hydrobenzoin, or hydrobenzoin-like diols, was first proposed by Yamamoto et al. in 1989[23] and subsequently employed by Rosini et al.[24] Later this procedure was also employed in the synthesis of bioactive sulfoxides[25] and of Omeprazole, or Omeprazole-like molecules.[26]

We used this protocol for the oxidation of aryl β-ketosulfides[18] and aryl benzyl sulfides[17,20–21] and we consistently observed a high enantioselectivity (*ee* in the range 91–>98%). In only a few cases were slightly lower values (*ee* in the range 81–88%) obtained.[20] Notably, as far as aryl benzyl sulfides were concerned,[20–21] this high enantioselectivity was obtained regardless of the nature, steric hindrance and position of various substituents on both aryl groups (Ar^1 and Ar^2 in Scheme 1).

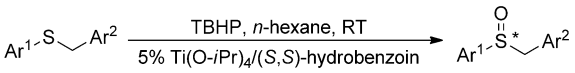

Scheme 1. Enantioselective oxidation of aryl benzyl sulfides with TBHP in the presence of a titanium/(*S*,*S*)-hydrobenzoin catalyst.

Interestingly, the oxidation of substrates differing in the structure from that of aryl benzyl sulfides, such as alkyl aryl sulfides, afforded a significantly lower enantioselectivity (52–62% *ee* values).[21] Similarly, Sulindac sulfides alkyl esters, that are precursors of bioactive molecules and are structurally similar to alkyl aryl sulfides, showed a lower enantioselectivity if oxidised by the same catalytic system.[19] From a synthetic point of view, the *ee* values obtained in the oxidation of these aryl alkyl sulfides could be increased if a kinetic resolution process in the over-oxidation of sulfoxide to sulfone was allowed.[19,21]

Recently, we also performed a combined computational-experimental study on the cited asymmetric oxidation of aryl benzyl sulfides bearing different substituents.[20] We used, as a model-system, unsubstituted benzyl phenyl sulfide reacting with *tert*-butyl hydroperoxide in the presence of complexes of titanium with (*S*,*S*)-hydrobenzoin and we found that the experimentally observed enantioselectivity depends on the relative energy of two preliminary octahedral titanium complexes that form in the first reaction phase. These complexes provide two diastereomeric pathways leading to (*R*)- and (*S*)-sulfoxide. The relative stability of these crucial intermediates was determined by the presence of weak interactions involving the aryl groups, in particular, aromatic CH···π interactions (also denoted in some cases as edge-to-face arene interactions or T-shaped CH···π interactions).[27–28] A schematic representation of the model-system used in ref. [20] is given in Figure 1. These weak interactions gained a recent interest mainly in crystal engineering research,[27] but they were also invoked to explain reaction mechanisms in asymmetric synthesis.[28]

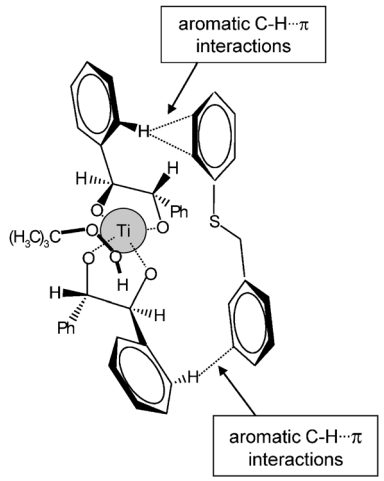

Figure 1. A schematic representation of the preliminary titanium complex involving two hydrobenzoin molecules, TBHP and the substrate sulfide.

In the present paper, we describe the unexpected behaviour observed in the case of fluoro-substituted benzyl phenyl sulfides. Although for partially fluorinated substrates we measured the usual excellent *ee* values (>98%), upon use of the same oxidation protocol on the substrate in which the aryl groups were completely fluorinated (pentafluorobenzyl pentafluorophenyl sulfide), we found for the first time a lower enantioselectivity (*ee* 61%). In light of our previous experimental results, this finding was rather surprising and not easy to explain on the basis of the previous computational model (i.e. existence and relative stability of preliminary titanium complexes). To check the reliability of our mechanistic hypothesis, we have examined two test-cases with the same DFT computational approach: 1) the oxidation of the sulfide in which the aryl groups were completely fluorinated (pentafluorobenzyl pentafluorophenyl sulfide) characterized by the unexpectedly lower *ee* and 2) the oxidation of a partially fluorinated substrate exhibiting the usual excellent *ee* (pentafluorobenzyl phenyl sulfide). Our aim was to answer the following questions: 1) does the topology of the reaction surface significantly change in the presence of a complete substrate fluorination? 2) Does the formation of the preliminary complexes remain the key-step in determining the preference for one of the two diastereomeric pathways? 3) Do the weak aromatic CH···π interactions still play a fundamental role in determining the relative energy of the two reaction channels? In both cases 1) and 2) the model-system is similar to that used in our previous study[20] and consists of the substrate molecule (pentafluorobenzyl pentafluorophenyl sulfide or pentafluorobenzyl phenyl sulfide), the *tert*-butyl hydroperoxide (TBHP) and the [(*S*,*S*)-hydrobenzoin]$_2$-Ti complex.

Results and Discussion

Experimental enantioselective oxidation: Reactivity of fluorinated aryl benzyl sulfides

In a previous paper, we performed the oxidation of *o*- and *p*-bromophenyl pentafluorobenzyl sulfide using TBHP in the presence of a complex of titanium and (*S*,*S*)- or (*R*,*R*)-hydrobenzoin. Our purpose was to investigate the effect of the complete fluorination of the phenyl moiety of the benzyl group on the reaction enantioselectivity.[21] As reported in the case of other differently substituted aryl benzyl sulfides,[17,20–21] we obtained the usual enantiopure sulfoxides (*ee* value >98%) in good isolated yields (81–97%).

However, upon use of the same protocol to oxidise pentafluorobenzyl pentafluorophenyl sulfide **1a**,[29] (i.e. the sulfide in which both phenyl rings are completely fluorinated), we obtained a low yield (19%) of the corresponding sulfoxide **1b** and a significantly lower enantioselectivity (61% *ee* value). Thus, after a series of examples of aryl benzyl sulfides that we have systematically oxidised with the same protocol to the corresponding sulfoxides with very high *ee* values,[17,20–21] we observed the first case of an unsatisfactory reactivity and a lower *ee* (Table 1, entry 1).

Table 1. Enantioselective oxidation of fluorinated aryl benzyl sulfides with TBHP in the presence of a titanium/(*S*,*S*)-hydrobenzoin complex.

Entry	Ar^1	Ar^2	Yield[a] [%]	*ee*[b] [%]
1	C_6F_5	C_6F_5	19	61[c] (*R*)[d]
2	C_6H_5	C_6F_5	91	>98 (*R*)[d]
3	2-F-C_6H_4	C_6F_5	96	>98 (*R*)[e]
4	C_6H_5	C_6F_5	86	>98 (*R*)[e]

[a] Yields refer to pure isolated products. [b] The *ee* values were measured by HPLC. [c] The *ee* value increased to 65% after crystallisation. [d] Configuration established by circular dichroism spectroscopy. [e] Configuration established by X-ray diffraction analysis.

In view of this unexpected result, we decided to examine other fluorinated aryl benzyl sulfides to provide a more reliable analysis of the reaction performance. Thus, we oxidised the pentafluorobenzyl phenyl sulfide **2a**,[30] that is, the sulfide in which only the phenyl moiety of the benzyl group is fluorinated and the other one bears no substituents. In this case, we obtained the usual enantiopure sulfoxide **2b**[31] (*ee* value >98%) in high isolated yield (91%; Table 1, entry 2). In a further experiment, we oxidised the 2-fluorophenyl pentafluorobenzyl sulfide **3a**, a substrate structurally similar to the already investigated[21] 2-bromophenyl pentafluorobenzyl sulfide, in which the bromine atom is replaced by the potentially more problematic fluorine one. In principle, this substitution close to the reaction centre could affect the reaction pathway, as reported in the case of the lower enantioselectivity observed if the methoxy group is present on the *ortho*- or *meta*-position of the phenyl group (84–88% *ee*).[20] However, even in case of sulfide **3a** (Table 1, entry 3), we obtained the usual enantiopure sulfoxide **3b** (*ee* value > 98%) in high isolated yield (96%). Finally, we performed the oxidation of benzyl pentafluorophenyl sulfide **4a**[32] (completely fluorinated non-benzyl phenyl group) and we found again a high isolated yield (86%; Table 1, entry 4) of the corresponding sulfoxides **4b**, obtained in enantiopure form (*ee* value >98%). These results indicate that only the simultaneous complete fluorination of both phenyl rings represents the structural feature responsible for the lower *ee* observed for sulfide **1a**.

Configurations and crystal structures of the enantiopure sulfoxides

On the basis of our previous work,[17–21] and in accordance with our earlier model,[20–21] (*R*)-sulfoxides **1b**–**4b** are the expected product if (*S*,*S*)-hydrobenzoin is used as a ligand of titanium. As we were not able to obtain suitable crystals of sulfoxide **2b** for X-ray diffraction experiments, we inferred its (*R*)-configuration on the basis of circular dichroism spectra. This approach provides highly reliable information for this class of molecules, as demonstrated in our recent theoretical and experimental papers on this topic[21,33]. Sulfoxide **2b** displayed the expected Mislow pattern[9] for the (*R*)-configuration, as shown in Figure S1 of the Supporting Information. Moreover, the same pattern was also shown by the enantioenriched sulfoxide **1b**, in which the predominant enantiomer should have the (*R*)-configuration too (Figure S1).

For sulfoxides **3b** and **4b** it was possible to assign the absolute configurations by X-ray diffraction experiments. We also observed the (*R*)-configuration in these cases. The crystal structures of **3b** and **4b** are depicted in Figure S2 and S3 (Supporting Information). The aryl groups of 2-fluorophenyl pentafluorobenzyl sulfoxide **3b** are arranged in a gauche conformation (dihedral angle = 65.0°), whereas the same moieties of the benzyl pentafluorophenyl sulfoxide **4b** are characterised by an anti periplanar conformation (dihedral angle = 179.6°). Furthermore, aryl groups are ordered into parallel displaced stacking structures,[34–35] a supramolecular arrangement which features molecules containing perfluorinated aryl groups.

Computational mechanistic study

The energy profile for the oxidation of the pentafluorobenzyl pentafluorophenyl sulfide by TBHP in the presence of the [(*S*,*S*)-hydrobenzoin]$_2$-Ti complex is shown in Figure 2. Schematic representations of the structure of the critical points located on the surface are reported in Figure 3–6. The asymptotic limit (AL) used as a reference in Figure 2 corresponds to the three non-interacting reactant molecules, that is the titanium(hydrobenzoin)$_2$ tetrahedral complex, the substrate pentafluorobenzyl pentafluorophenyl sulfide and TBHP, at infinite distance. At the beginning of the process, the approaching of substrate to the titanium complex affords two different intermediates **M1** and **M1'**, depending on the relative orientation of the two molecules. As found in our previous work,[20] the subsequent interaction with TBHP does not require any activation barrier and gives two new intermediate species **M2** and **M2'** in which the

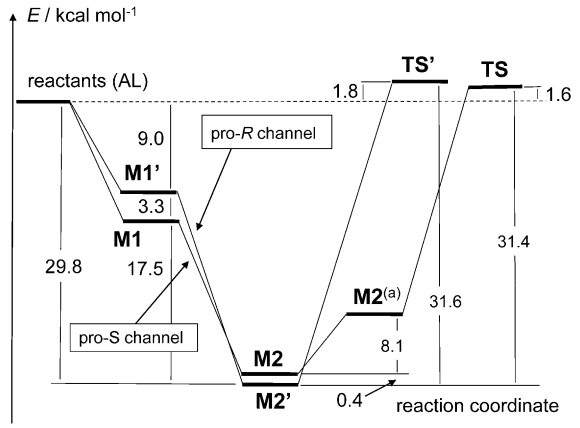

Figure 2. Computed energy profile for the enantioselective oxidation of pentafluorobenzyl pentafluorophenyl sulfide **1 a** in the presence of the [(*S*,*S*)-hydrobenzoin]$_2$-Ti catalyst.

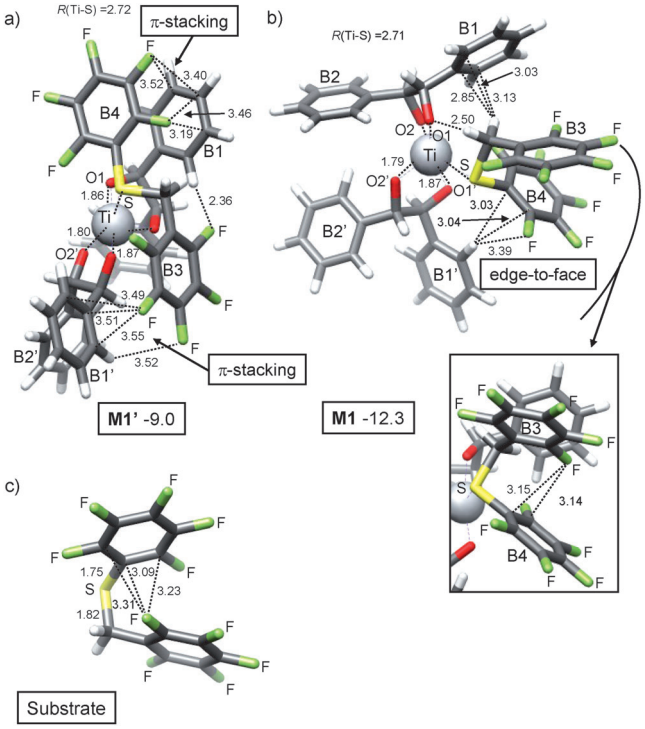

Figure 3. A schematic representation of the structures of the two diastereomeric titanium pentacoordinate adducts a) **M1'** and b) **M1** for pentafluorobenzyl pentafluorophenyl sulfide **1 a** and c) the substrate. Bond lengths (*R*) are in [Å], energies in [kcal mol^{-1}] relative to AL.

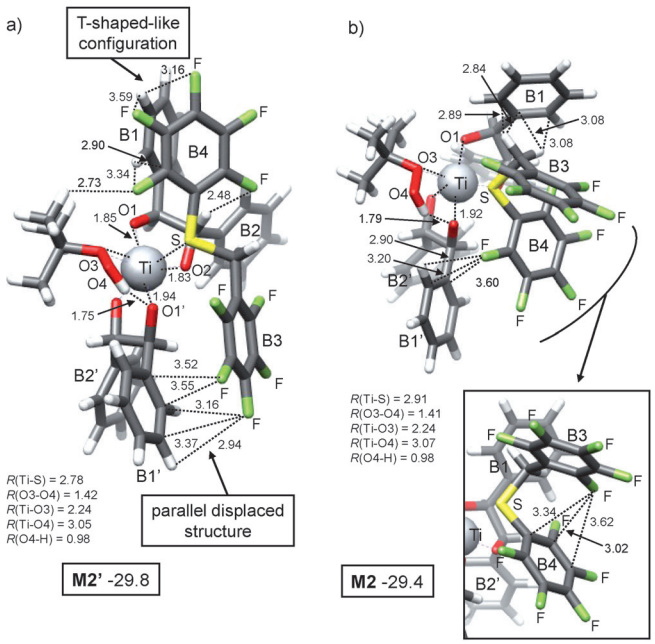

Figure 4. A schematic representation of the structure of the two diastereomeric octahedral titanium complexes a) **M2'** and b) **M2** for pentafluorobenzyl pentafluorophenyl sulfide **1 a**. Bond lengths (*R*) are in [Å], energies in [kcal mol^{-1}] relative to AL.

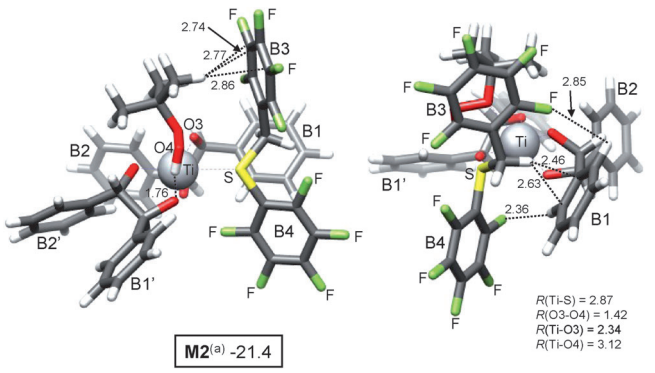

Figure 5. A schematic representation of the structure of the octahedral titanium complexes complex **M2**$^{(a)}$ for pentafluorobenzyl pentafluorophenyl sulfide **1 a**. Bond lengths (*R*) are in [Å], energies in [kcal mol^{-1}] relative to AL.

peroxide group is oriented toward the sulfur atom. Along the reaction path which stems from **M1**, we have located an additional critical point **M2**$^{(a)}$, which differs from **M2** in the conformation of the substrate molecule. **TS** and **TS'** are transition states in which an oxygen atom moves from the peroxide group to sulfur to form the final sulfoxide species. As the two reaction pathways **M1**→**M2**→**TS** and **M1'**→**M2'**→**TS'** afford a final sulfoxide product with configuration *S* and *R* at the sulfur atom, respectively, they are denoted in Figure 2 as pro-*S* and pro-*R* channel.

Even if this energy profile is qualitatively similar to that computed in our previous investigation, in which a non-fluorinated substrate (i.e. benzyl phenyl sulfide) was used as a model-system,[20] important differences in the comparison between the two reaction surfaces can be detected. The new profile shows an increase of the energy gap between the two preliminary complexes **M1** and **M1'**. This quantity, which was 1.7 kcal mol^{-1} for benzyl phenyl sulfide, is now 3.3 kcal mol^{-1}. However, the major and most important change caused by complete substrate fluorination is found in the **M2**–**M2'** energy gap: although in the non-fluorinated case **M2'** was 5.1 kcal mol^{-1} lower in energy than **M2**, these two adducts are almost degenerate in this experiment (the difference is only 0.4 kcal mol^{-1}, with **M2'** more stable than **M2**). The secondary minimum **M2**$^{(a)}$

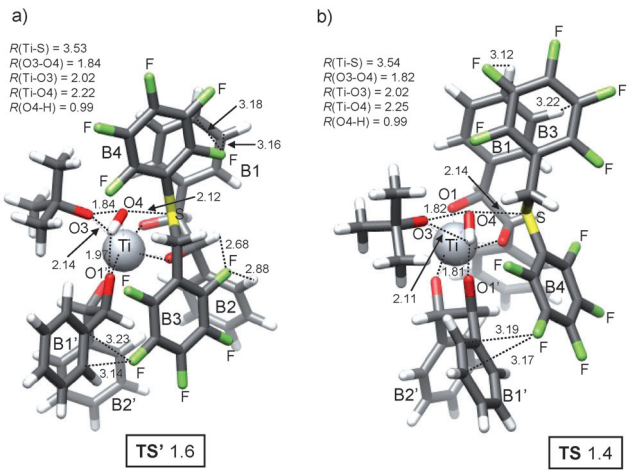

Figure 6. A schematic representation of the structure of the two diastereomeric transition states a) **TS'** and b) **TS** for pentafluorobenzyl pentafluorophenyl sulfide **1 a**. Bond lengths (*R*) are in [Å], energies in [kcal mol^{-1}] relative to AL.

is 8.1 kcal mol^{-1} higher than **M2**. No significant variation was found in the relative energy of the two transition states **TS** and **TS',** which are almost degenerate (as found in our previous study), their energy difference being only 0.2 kcal mol^{-1}. However, in the present case they lie slightly above the asymptotic limit, **TS** being 1.6 kcal mol^{-1} higher than AL.

The near degeneracy of **M2** and **M2'**, which are the lowest energy minima along the two reaction channels, has important effects on the enantioselectivity of the reaction. As pointed out in our previous work,[20] the *ee* is determined by the energetics and kinetic features of the first phase of the reaction affording **M2** and **M2'**. Owing to their near degeneracy, these two adducts should form in similar amounts. Also, because the two transition states are very close in energy, the two corresponding reaction channels are both significantly populated and the relative yield of the two final products (differing in sulfur configuration) must be similar, in agreement with the lower *ee* experimentally observed.

Our aim is now to understand the structural and electronic factors that, upon complete fluorination of the two substrate benzene rings, affect the relative energy of the intermediate adducts (**M1** compared to **M1'**, **M2** compared to **M2'**, and **M2**$^{(a)}$ compared to **M2**) and transition states (**TS** and **TS'**). Inspection of Figure 3 shows that the two penta-coordinated titanium complexes **M1** and **M1'** significantly differ in the way the benzene rings of the hydrobenzoin ligands (B1, B2, B1′ and B2′) interact with the substrate. More precisely, the structural features of **M1'** are rather similar to those already outlined for the corresponding complex in the non-fluorinated case.[20] The substrate has roughly a linear structure that allows the activation of π-stacking interactions (as shown in Figure 3 a) between the perfluorophenyl rings of the substrate (B3 and B4) and the phenyl rings B1 and B1′ of both hydrobenzoin ligands. However, because of the presence of fluorine atoms on both substrate rings, the nature and strength of these interactions differ from those discussed in our earlier study. In the present case, the planes of the interacting rings are approximately planar for both phenyl pairs (B1-B4 and B1′-B3), but they are displaced in such a way that an electron-rich fluorine atom of the substrate can interact with the carbon atoms of the hydrobenzoin phenyl group. This parallel-displaced arrangement is the most favourable one,[34–35] as demonstrated in accurate computational studies by Tsuzuki et al.[36] Typical F–C distances that feature these interactions are in the range 3.2–3.5 Å, as shown in Figure 3 a; these values are in agreement with those reported in literature.[34–35] In addition to the previously cited interactions, a hydrogen bond involving a B3 fluorine atom and a B1 C–H bond contributes to the stabilisation **M1'** (the computed (B1)C–H···F(B3) distance is 2.36 Å). This value is in rather good agreement with the H···F distance found in the crystal structure of some fluorobenzenes characterized by the presence of this type of hydrogen bonds.[37–38]

In **M1** (see Figure 3 b), the substrate abandons the linear conformation that characterises **M1'** and adopts a bent conformation, which is almost identical to that of the isolated substrate (depicted in Figure 3 c). As a consequence, the interaction pattern between the substrate and the two hydrobenzoin ligands completely changes with respect to **M1'** and the analogous **M1** complex found in the case of benzyl phenyl sulfide.[20] In the present case, the fluorinated rings form a sort of displaced "sandwich" structure in which one electron-rich fluorine atom of ring B3 can effectively interact with two electron-poor carbon atoms of ring B4 (an extra partial perspective of **M1** is provided in Figure 3 b to illustrate these interactions). The nature of these F···C interactions is only apparently similar to that previously discussed for **M1'**. In **M1** they are expected to be more effective because the carbon atoms are now electron-poorer than in the previous case, each carbon atom being bonded to a fluorine atom. Thus, they can be considered to be real strong π-donor/π-acceptor interactions. Their augmented strength, as a result of the complete fluorination of the phenyl groups, is confirmed by the shorter F–C distances computed for the B3-B4 pair (3.14 and 3.15, as shown in Figure 3 b) with respect to the values obtained for the B4-B1 pair in **M1'** (3.19 and 3.40 Å are the shortest (B4)F···C(B1) distances computed in that case). Notably, these values are in good agreement with the shortest distances between stacked fluorinated phenyl rings found in the crystal structures of sulfoxides **3 b** and **4 b**.

Two additional important interactions have been revealed by our computations on **M1**. One interaction is given by an edge-to-face (or T-shaped) configuration[27–28,34] involving the ring pair B1′-B4. In this edge-to-face structure, which is made possible by the particular "folded" substrate arrangement, the plane of the hydrobenzoin phenyl ring B1′ is roughly orthogonal to the plane of the substrate ring B4 (3.03 and 3.04 Å are the shortest distances between one (B1′)C–H bond and the B4 carbon atoms). This structure was demonstrated to be more stabilising than "parallel-displaced" and "sandwich" structures because of the additional contribution of H-bonding.[34–36] In the present case the C–H bond points to the middle of a (B4)C–C bond (C–H···π interaction) and interacts at the same time with an electron-rich fluorine atom (C–H···F distance = 3.39 Å). This value is longer with respect to crystallographic data[37–38] and that previously found in **M1'**. This difference is

probably a result of the particular edge-to-face arrangement of the two rings B1′ and B4 and the simultaneous presence of other interactions. The other interaction involves the substrate methylene group, the B1 benzene ring and one hydrobenzoin oxygen O1. Inspection of Figure 3b shows that one of the C–H methylene bonds points toward B1: the computed distances between this (methylene)C–H bond and three B1 carbon atoms (2.85, 3.03 and 3.13 Å) indicate a non-negligible interaction of the C–H bond with the π-electron cloud of B1 (C–H···π interaction). The second (methylene)C–H bond is involved into a hydrogen interaction with the hydrobenzoin O1 oxygen, the (methylene)C–H···O1 distance being 2.50 Å. This computational finding suggests that the particular displaced "sandwich" structure that features the substrate in the **M1** complex (which allows a significant interaction between the two rings B3 and B4) and the interaction of the substrate methylene group with B1 and O1, are the factors responsible for the energy lowering of **M1** and the augmented **M1**–**M1′** energy gap (from 1.7 in the non-fluorinated molecule to 3.3 kcal mol^{-1} in the present case).

Particularly important now is to elucidate the factors that determine the near degeneracy of **M2** and **M2′**. Inspection of Figure 4 shows that in **M2′** the substrate maintains the approximately linear conformation of **M1′** and the resulting structure is apparently similar to that obtained in the non-fluorinated case.[20] However, a more detailed analysis shows that the presence of fluorine atoms is responsible for some important structural changes. Upon addition of TBHP, one hydrobenzoin molecule is pushed closer to the substrate and the B1 ring rotates around the C–C bond to make room in the metal coordination sphere. As a consequence of this rotation, the most effective interactions between B1 and B4 are now determined by a relative arrangement of the two rings similar to an edge-to-face configuration (or T-shaped-like), even if the B1 and B4 planes form a dihedral angle much lower than 90°. As a result of the complete fluorination, the (B1)C–H bonds approximately point towards two electron-rich fluorine atoms on B4: 3.34 and 3.16 Å are the shortest (B1)C–H···F(B4) computed distances. Furthermore, an important hydrogen bond has been detected between one B4 fluorine atom and one hydrogen of the hydrobenzoin methylene unit adjacent to B2, the (B4)F···H-C(methylene) distance being 2.48 Å. An additional significant interaction involves another B4 fluorine atom and the hydrogen atom of a methyl group of TBHP (the computed (B4)F···H–C(methyl) distance is 2.73 Å). The relative arrangement of the two rings B1′ and B3 is analogous to that found in **M1′.** These two rings form a parallel-displaced structure in which an electron rich fluorine atom of B3 interacts with two electron-poor carbon atoms of B1′: the shortest (B3)F···C(B1′) distances are 3.16 and 3.37 Å, which are close to the values found in **M1′**.

If we neglect the approaching TBHP molecule (responsible for the new octahedral configuration of titanium), the structure of **M2** (see Figure 4b) closely resembles that of **M1**: the substrate is again characterised by the bent conformation ("displaced sandwich-structure") in which electron-rich fluorine atoms of B3 interact with electron-poor carbon atoms of B4 (the shortest (B3)F···C(B4) distances are 3.02 and 3.34 Å, as reported in the bottom part of Figure 4b). Furthermore, since the hydrobenzoin molecule is pushed apart by the entering TBHP, the substrate methylene is now too far away to maintain the hydrogen bond with O1. However, to compensate the loss of this stabilising interaction, both C–H bonds of the substrate methylene now effectively interact with the B1 π electron cloud (C–H···π interaction), as demonstrated by the (methylene)C–H···C(B1) distances reported in the Figure (2.89 and 2.84 Å are characteristic values). A further important interaction revealed by our computations (and which differentiates this **M2** structure from that computed in the non-fluorinated case of ref. 20) is the interaction between a B4 fluorine atom and a hydrogen atom on B1′, the B(4)F···H–C(B1′) distance being 2.90 Å. On the basis of our analysis, it is reasonable to believe that the "displaced sandwich-conformation" of the substrate is the key factor that determines the energy lowering of **M2** and the consequent near degeneracy of the two intermediates **M2′** and **M2**. It is important to outline that the other stabilising interactions detected in **M2** (i.e. the interaction of the substrate methylene C–H bonds with B1 and the hydrogen interaction B(4)F···H–C(B1′)) are a consequence of the particular bent conformation of the substrate molecule.

Our analysis concerning the factors that are responsible for the stabilisation of **M2** is confirmed by the existence of an additional structure (showing the same substrate orientation that features **M2**) in which the substrate molecule maintains the linear conformation found in **M2′**. Since in the subsequent transition state **TS** the substrate has a linear conformation, this secondary minimum (denoted as **M2**$^{(a)}$) must represent an intermediate belonging to the pro-*S* channel (**M1**→**M2**→**M2**$^{(a)}$→**TS**). The formation of **M2**$^{(a)}$ after "substrate unfolding" allows the reacting system to enter the transition region. **M2**$^{(a)}$, which lies 8.1 kcal mol^{-1} higher in energy with respect to **M2**, is schematically represented in Figure 5 in two different perspectives. Interestingly, the **M2**$^{(a)}$–**M2** energy gap is not very different from that between **M2′** and **M2** computed in the non-fluorinated case (5.1 kcal mol^{-1}) in which **M2** was characterised by a linear conformation.[20] This result unambiguously points to the "sandwich" structure (or "folded" conformation) of the substrate molecule as the key factor that stabilises **M2**.

In the transition state **TS**, as previously outlined, the distinctive "sandwich" structure that stabilises **M1** and **M2**, disappears. In both **TS** and **TS′** (see Figure 6), that are almost degenerate, the substrate molecule is approximately linear and the arrangement of the various ligands around the metal is rather similar to that found in the non-fluorinated case.[20] We believe it is important to point out again that the **TS** structure unambiguously indicates that the secondary minimum **M2**$^{(a)}$ (in which the substrate has attained a linear conformation) represents a "necessary" conformational arrangement that must be adopted by the reacting system before reaching the transition state region. In Figure 6, we have highlighted the migrating O4 oxygen atom, the breaking O3-O4 bond (1.84 and 1.82 Å in **TS′** and **TS**, respectively) and the new forming O4–S bond (2.12 and 2.14 Å). During the migration, the O4 bonded hydrogen atom moves closer to O3 and, in both **TS** and **TS′**, forms a strong hydrogen bond that anticipates the O3–H bond in

the final product (the O4-H···O3 distance is 2.14 and 2.11 Å in **TS'** and **TS**, respectively). Notably, if O4 moves from O3 to S and the hydrogen atom comes nearer to O3, the hydrogen-bond between this hydrogen atom and O1' is maintained in the transition structures, which helps to stabilises the migration pathway.

In addition to the oxidation of the completely fluorinated sulfide **1a**, we investigated also the case of the pentafluorobenzyl phenyl sulfide **2a**, that was oxidised with the same procedure yielding the enantiopure sulfoxide **2b**. Since the key features of the surface determining the enantioselectivity of the reaction are the relative energies of the **M2**- and **M2'**-type intermediates and **TS** and **TS'** transition states, we focused our investigation on these two regions of the potential surface, which is depicted in Figure 7. As previously found, in the inter-

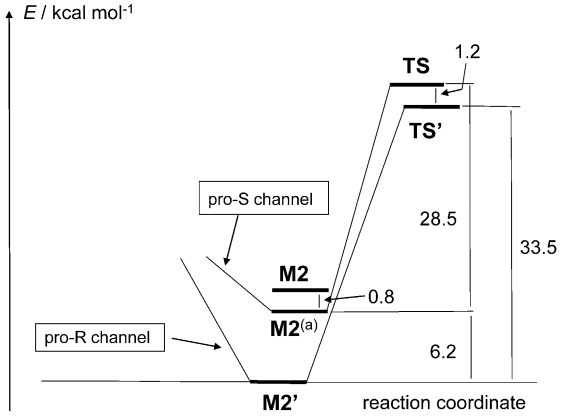

Figure 7. Computed energy profile for the enantioselective oxidation of pentafluorobenzyl phenyl sulfide **2a** in the presence of the [(*S*,*S*)-hydrobenzoin]$_2$-Ti catalyst.

mediate region we have located two critical points **M2** and **M2**$^{(a)}$, again differing in the conformation of the substrate molecule (**M2** and **M2**$^{(a)}$ denote, as in the previous discussion, the two structures with "folded" and "unfolded" linear conformation of the substrate, respectively). The most significant change caused by the partial substrate fluorination (only the phenyl ring of the benzyl group is fluorinated) is given by the variation of the energy difference between the **M2-** and **M2'**-type intermediates. In this case, the two adducts are no longer degenerate and **M2'** is 6.2 kcal mol^{-1} lower in energy than **M2**$^{(a)}$. Interestingly, this value is close to that previously found,[20] for benzyl phenyl sulfide (5.1 kcal mol^{-1}). The other minimum **M2** (folded substrate structure) is 0.8 kcal mol^{-1} higher than **M2**$^{(a)}$. Furthermore, the two transition states are again close in energy, **TS'** being only 1.2 kcal mol^{-1} lower than **TS**. The resulting energy diagram (almost identical to that reported in ref. [20]) for the non-fluorinated substrate, suggests that the **M2'** adducts forms almost exclusively during the first reaction phase and the dominant reaction channel is the one affording configuration *R* (pro-*R* channel) at the sulfur atom in the sulfoxide product, in agreement with the experimental evidence.

A schematic representation of **M2'**, **M2** and **M2**$^{(a)}$ is given in Figure S4 of the Supporting Information. The structure of **M2'** is very similar to the corresponding structure found for pentafluorobenzyl pentafluorophenyl sulfide: the substrate is characterised by a linear conformation and similar interactions involving the two ring pairs B3 and B1' and B1 and B4 can be recognised. The most interesting result concerns **M2** and **M2**$^{(a)}$, that is, the two structures differing in the substrate conformation. Unlike the results obtained for the completely fluorinated sulfide, in this case the more stable structure is **M2**$^{(a)}$, which is featured by a linear conformation of the substrate while the "sandwich" folded conformation is found in **M2**.

This computational finding, which is reversed with respect to that found for pentafluorobenzyl pentafluorophenyl sulfide **1a**, indicates that, in the presence of a partial fluorination of the substrate, the folded "sandwich" structure does not stabilise **M2** strongly enough to make it degenerate to **M2'**. The factors that make the sandwich conformation less effective in stabilising **M2** are evident from the analysis of Figure S4c (Supporting Information). The lacking of fluorine atoms on the phenyl ring (B4) partly cancels the strong stabilising interactions between one B4 fluorine atom and the ring B1': in particular the hydrogen bond between fluorine and a B1' ring hydrogen definitely disappears. Finally, no significant differences are evident in the comparison of **TS** and **TS'** to the corresponding transition structures found for the completely fluorinated substrate (see Figure S5 of the Supporting Information). The small energy gap between the two transition states confirms that the interaction pattern does not change significantly.

Conclusions

We performed a combined computational and experimental study of the oxidation of fluorinated aryl benzyl sulfides using *tert*-butyl hydroperoxide (TBHP) in the presence of a complex between titanium and (*S*,*S*)-hydrobenzoin. In a framework characterised by an invariantly high enantioselective oxidation (*ee* values $>98\%$), the particular case of pentafluorobenzyl pentafluorophenyl sulfide **1a** emerged as the only exception, for which the oxidation was characterised by a lower enantioselectivity (61% *ee* value). To explain this unexpected stereochemical result, we examined the reaction potential energy surface at the DFT level for two test-cases: 1) the pentafluorobenzyl phenyl sulfide, which shows the usual excellent *ee* value and 2) the pentafluorobenzyl pentafluorophenyl sulfide characterised by a less satisfactory enantioselectivity. To this purpose we used a model-system formed by the substrate molecule, the oxidant TBHP and the [(*S*,*S*)-hydrobenzoin]$_2$-Ti complex. The model-system is identical to that employed in a previous work to rationalise the results for other substituted aryl benzyl sulfides.

As discovered in our previous study, we found that the enantioselectivity is governed by the relative energy of the two octahedral complexes that form if the oxidant approaches the initial complex between [(*S*,*S*)-hydrobenzoin]$_2$-Ti and the substrate. These octahedral complexes form in the first reaction phase before the oxygen transfer. They are diastereomers

differing in the orientation of the substrate with respect to the metal and the oxidant. Two distinct diastereomeric pathways stem from these complexes and lead to the two sulfoxides that differ in the configuration of the newly formed sulfur chiral centre.

In the case of pentafluorobenzyl pentafluorophenyl sulfide the two octahedral complex intermediates are almost degenerate (their energy difference is only 0.4 kcal mol^{-1}) and they should form in similar amounts. Since the two transition states that originate from these intermediate species are very close in energy, the probabilities to follow one or the other diastereomeric reaction channel (pro-*R* or pro-*S*) become comparable, which leads to the lower experimentally observed enantiomeric excess.

Our computations indicate that the "displaced sandwich-conformation" of the substrate is the key factor that determines the energy lowering of **M2** and the consequent near degeneracy of **M2** and **M2'**. Furthermore, other stabilising interactions detected in **M2** (i.e. the interaction of the substrate methylene C–H bonds with the π cloud of ring B1 and the hydrogen interaction B(4)F···H-C(B1') are a consequence of the unusual and unexpected bent conformation of the substrate moiety.

For pentafluorobenzyl phenyl sulfide we found that the complex leading to configuration *R* (**M2'**) is significantly more stable than that affording configuration *S* (**M2**), the energy gap being 6.2 kcal mol^{-1}. As pointed out in the above discussion, the *ee* is determined by the energetics and kinetic features of the first reaction phase affording **M2** and **M2'**. Thus, because **M2'** is much more populated than **M2**, the reacting system preferentially follows the pathway that originates from the more stable intermediate, leading to the (*R*) configuration at the sulfur stereogenic centre.

Our computations clearly indicate that if the substrate is only partially fluorinated the folded "sandwich" structure does not stabilise **M2** strongly enough to make it degenerate to **M2'** and the arrangement of **M2** becomes similar to that observed for other phenyl benzyl sulfides.[20] In particular, the lacking of fluorine atoms on the sulfide phenyl ring cancels the strong stabilising interactions observed in the pentafluorobenzyl pentafluorophenyl sulfide between one phenyl fluorine atom and one hydrobenzoin phenyl ring. These results are further evidence of the value and reliability of the computational model that we proposed in a previous paper[20] to explain the persistent high enantioselectivity found in the catalysed oxidation of a large series of differently substituted aryl benzyl sulfides.

Experimental Section

Chemicals were purchased from Sigma–Aldrich and were used as received. *n*-Hexane employed in the enantioselective oxidation protocol was distilled from 4 Å molecular sieves prior to use. NMR spectra were recorded by using a Bruker AM500 spectrometer. HPLC analyses were performed on a Agilent 1100 chromatograph, equipped with a DAD detector. Elemental analyses were performed by using a Carlo Erba CHNS-O EA1108 elemental analyser. Circular dichroism spectra were recorded in acetonitrile solution by using a Jasco J-810 spectropolarimeter.

Sulfides **2a**–**4a** were synthesised by standard reaction of the corresponding benzyl bromides in acetone with the sodium salt of commercially available thiols at 50 °C. Sulfide **1a** was obtained by reacting for 18 h pentafluorothiophenol with triethylamine and pentafluorobenzyl bromide in acetone at −20 °C to avoid the formation of large amounts of side products.

Syntheses and Characterisation data

Pentafluorobenzyl pentafluorophenyl sulfide (**1a**):[29] M.p. 73–74 °C (*n*-hexane).

Pentafluorobenzyl phenyl sulfide (**2a**):[30] Kugelrohr oven temp 90–92 °C, $p = 0.1$ mbar.

2-Fluorophenyl pentafluorobenzyl sulfide (**3a**): Kugelrohr oven temp 85–88 °C, $p = 0.1$ mbar. ^{1}H NMR (500 MHz, $CDCl_3$): $\delta = 7.36$–7.30 (m, 2H, H_{Ar}), 7.12–7–08 (m, 1H, H_{Ar}), 7.07–7.03 (m, 1H, H_{Ar}), 4.08 ppm (t, $^4J_{H,F} = 1.2$ Hz, 2H, CH_2); ^{13}C NMR (125 MHz, $CDCl_3$): $\delta =$ 162.9 (d, $^1J_{C,F} = 248$ Hz, C_{Ar}), 144.9 (d-like, $^1J_{C,F} = 256$ Hz, C_{Ar}), 140.4 (d-like, $^1J_{C,F} = 254$ Hz, C_{Ar}), 137.2 (d-like, $^1J_{C,F} = 255$ Hz, C_{Ar}), 135.8 (C_{Ar}), 131.1 (d, $^3J_{C,F} = 8.3$ Hz, C_{Ar}), 124.5 (d, $^3J_{C,F} = 3.5$ Hz, C_{Ar}), 120.0 (d, $^2J_{C,F} = 18.7$ Hz, C_{Ar}), 116.0 (d, $^2J_{C,F} = 22.9$ Hz, C_{Ar}), 112.3 (m, C_{Ar}), 26.0 ppm (CH_2); elemental analysis calcd (%) for $C_{13}H_6F_6S$: C 50.65, H 1.96; found: C 50.70, H 2.22.

Benzyl pentafluorophenyl sulfide (**4a**):[32] Kugelrohr oven temp 83–85 °C, $p = 0.1$ mbar.

Racemic sulfoxides **1b**–**4b** (used in the setting up of the chiral HPLC separation) were synthesised by standard mCPBA oxidation. Enantioenriched sulfoxides **1b**–**4b** were produced by the TBHP-oxidation according to our protocol[17–21] in *n*-hexane, in the presence of 5 mol% of titanium/hydrobenzoin catalyst (see also Supporting Information).

Pentafluorobenzyl pentafluorophenyl sulfoxide (**1b**): M.p. 133–135 °C (*n*-hexane/ethanol 1:1). $[\alpha]_D^{25} = +23.3$ ($c = 0.8$, $CHCl_3$) for a sulfoxide with an *ee* of 65%; ^{1}H NMR (500 MHz, $CDCl_3$): $\delta = 4.69$–4.68 ppm (m, 2H, CH_2); ^{13}C NMR (125 MHz, $CDCl_3$): $\delta = 145.7$ (d-like, $^1J_{C,F} = 251$ Hz, C_{Ar}), 145.4 (d-like, $^1J_{C,F} = 256$ Hz, C_{Ar}), 144.1 (d-like, $^1J_{C,F} = 260$ Hz, C_{Ar}), 143.7 (d-like, $^1J_{C,F} = 257$ Hz, C_{Ar}), 137.7 (d-like, $^1J_{C,F} = 254$ Hz, C_{Ar}), 116.4 (m, C_{Ar}), 103.4 (m, C_{Ar}), 47.2 ppm (CH_2); elemental analysis calcd (%) for $C_{13}H_2F_{10}OS$: C 39.41, H 0.51; found: C 39.54, H 0.61; the *ee* value was measured by HPLC (Column: Chiralcel OD-H. Eluent: hexane/*i*-propanol 70:30).

Pentafluorobenzyl phenyl sulfoxide (**2b**):[31] M.p. 169–171 °C (*n*-hexane/ethanol 8:2). $[\alpha]_D^{25} = +190.7$ ($c = 1.1$, $CHCl_3$). The *ee* value was measured by HPLC (Column: Whelk-O1. Eluent: hexane/*i*-propanol 90:10).

2-Fluorophenyl pentafluorobenzyl sulfoxide (**3b**): M.p. 103–105 °C (*n*-hexane/acetone 8:2). $[\alpha]_D^{25} = +278.6$ ($c = 1.1$, $CHCl_3$); ^{1}H NMR (500 MHz, $CDCl_3$): $\delta = 7.57$–7.51 (m, 2H, H_{Ar}), 7.35–7.31 (m, 1H, H_{Ar}), 7.18–7.12 (m, 1H, H_{Ar}), 4.42 (d, $^2J_{H,H} = 13.3$ Hz, 1H, CH_2), 4.27 ppm (d, $^2J_{H,H} = 13.3$ Hz, 1H, CH_2); ^{13}C NMR (125 MHz, $CDCl_3$): $\delta = 158.0$ (d, $^1J_{C,F} = 247$ Hz, C_{Ar}), 145.8 (d-like, $^1J_{C,F} = 247$ Hz, C_{Ar}), 141.2 (d-like, $^1J_{C,F} = 256$ Hz, C_{Ar}), 137.3 (d-like, $^1J_{C,F} = 254$ Hz, C_{Ar}), 133.7 (d, $^3J_{C,F} =$ 7.6 Hz, C_{Ar}), 129.5 (d, $^2J_{C,F} = 16.6$ Hz, C_{Ar}), 125.9 (d, $^4J_{C,F} = 2.1$ Hz, C_{Ar}), 125.3 (d, $^3J_{C,F} = 3.5$ Hz, C_{Ar}), 115.7 (d, $^2J_{C,F} = 20.1$ Hz, C_{Ar}), 103.7 (m, C_{Ar}), 47.8 ppm (CH_2); the *ee* value was measured by HPLC (Column: Whelk-O1. Eluent: hexane/*i*-propanol 90:10); elemental analysis calcd (%) for $C_{13}H_6F_6OS$: C 48.16, H 1.87; found: C 47.96, H 1.61.

Benzyl pentafluorophenyl sulfoxide (4b): M.p. 115–117 °C (*n*-hexane); $[\alpha]_D^{25} = -64.0$ ($c = 0.6$, $CHCl_3$); ^1H NMR (500 MHz, $CDCl_3$): $\delta = 7.37–7.28$ (m, 3H, H_{Ar}), 7.20–7.14 (m, 2H, H_{Ar}), 4.68 (d, $^2J_{H,H} = 12.4$ Hz, 1H, CH_2), 4.53 ppm (d, $^2J_{H,H} = 12.4$ Hz, 1H, CH_2); ^{13}C NMR (125 MHz, CD_3COCD_3): $\delta = 147.2$ (d-like, $^1J_{C,F} = 250$ Hz, C_{Ar}), 143.2 (d-like, $^1J_{C,F} = 250$ Hz, C_{Ar}), 139.5 (d-like, $^1J_{C,F} = 255$ Hz, C_{Ar}), 132.2 (C_{Ar}), 131.4 (C_{Ar}), 130.7 (C_{Ar}), 130.5 (C_{Ar}), 119.7 (C_{Ar}), 62.0 ppm (CH_2); the *ee* value was measured by HPLC (Column: Chiralcel OD-H. Eluent: hexane/*i*-propanol 70:30); elemental analysis calcd (%) for $C_{13}H_7F_5OS$: C 50.98, H 2.30; found: C 50.80, H 2.53.

X-Ray data for suitable crystals were collected at 293 K by means of Nonius Kappa CCD single crystal X-ray diffractometer. Unit cell parameters are reported in Table S1 (Supporting Information). Data collection[39] was subjected to Lorentz, polarisation and absorption effects correction.[40] The structures were solved by direct methods procedure of SIR97,[41] and refined, for all unique measured data, by full-matrix-least-square on F^2 (FMLS) technique of SHELXL-97.[42] Non-hydrogen atoms were refined using anisotropic displacement parameters. Hydrogen atoms were located by means of Fourier maps application, and were refined with the isotropic displacement parameter (U_{iso}); hydrogen atoms of phenyl ring within **3b** structure were geometrically imposed with riding model constraints (C–H_{Ar} 0.93 Å, with $U_{iso}(H) = 1.2\,U_{iso}(C)$). CCDC 876025 (**3b**) and CCDC 876664 (**4b**) contains the supplementary crystallographic data for this paper. These data can be obtained free of charge from the Cambridge Crystallographic Data Centre at www.ccdc.cam.ac.uk/data_request/cif.

Computational methods

As the investigated model-system involves aryl groups in the substrate and ligands, it is reasonable to believe that a reliable estimate of interactions involving π systems (π–π stacking interactions, T-shaped interactions) is essential in the computation of the potential surface. It is well known that this class of interactions cannot be correctly treated at the DFT level because the most popular functionals (for instance, B3LYP) are inaccurate for interactions in which medium-range correlation effects are dominant such as aromatic-aromatic stacking.[43] The MP2 method can satisfactorily describe these interactions but, given the size of the model-system used here, these computations would require too much computational time for a practical and extensive usage. However, a new hybrid functional (denoted as MPWB1K), which is capable of treating medium-range correlation effects, has been proposed.[44] This functional has been demonstrated to provide a good estimate of the π–π interactions and reaction energetic[45–46] using reasonable amounts of computational time. Thus, all DFT computations reported in the present paper, have been performed with the Gaussian 03 series of programs[47] using the MPWB1K[44] functional and the DZVP basis set.[48] The DZVP basis is a local spin density optimised basis set of double-zeta quality that includes polarisation functions and is suitable to describe weak hydrogen and π interactions such as those occurring in the system investigated here. The transition vector of the various transition states has been analysed by means of frequency computations.

Acknowledgements

We thank Dr. Giuseppe Fracchiolla (Dipartimento Farmaco-Chimico, Università di Bari, Italy) for acquiring circular dichroism spectra and Mr. Giuseppe Chita (CNR, Istituto di Cristallografia, Bari, Italy) for X-ray data collection.

Keywords: density functional calculations · enantioselectivity · oxidation · reaction mechanisms · titanium

[1] E. Wojaczyńska, J. Wojaczyński, *Chem. Rev.* **2010**, *110*, 4303–4356.
[2] I. Fernández, N. Khiar, *Chem. Rev.* **2003**, *103*, 3651–3705; H. Pellissier, *Tetrahedron* **2006**, *62*, 5559–5601.
[3] M. C. Carreño, *Chem. Rev.* **1995**, *95*, 1717–1760.
[4] C. Bolm, K. Muñiz, J. P. Hildebrand in *Comprehensive Asymmetric Catalysis*, (Eds.: E. N. Jacobsen, A. Pfalz, H. Yamamoto), Springer, Berlin, **1999**, pp. 697–710.
[5] R. Bentley, *Chem. Soc. Rev.* **2005**, *34*, 609–624.
[6] H. Cotton, T. Elebring, M. Larsson, L. Li, H. Sorensen, S. von Unge, *Tetrahedron: Asymmetry* **2000**, *11*, 3819–3825.
[7] M. Seenivasaperumal, H.-J. Federsel, K. J. Szabó, *Adv. Synth. Catal.* **2009**, *351*, 903–919.
[8] K. K. Andersen, *Tetrahedron Lett.* **1962**, *3*, 93–95; K. K. Andersen, W. Gaffield, N. E. Papanikolaou, J. W. Foley, R. I. Perkins, *J. Am. Chem. Soc.* **1964**, *86*, 5637–5646.
[9] K. Mislow, M. M. Green, P. Laur, J. T. Melillo, T. Simmons, A. L. Ternay, Jr., *J. Am. Chem. Soc.* **1965**, *87*, 1958–1976.
[10] F. Di Furia, G. Modena, R. Seraglia, *Synthesis* **1984**, 325–326.
[11] P. Pitchen, H. B. Kagan, *Tetrahedron Lett.* **1984**, *25*, 1049–1052; P. Pitchen, E. Duñach, M. N. Desmukh, H. B. Kagan, *J. Am. Chem. Soc.* **1984**, *106*, 8188–8193.
[12] J. Legros, J. R. Dehli, C. Bolm, *Adv. Synth. Catal.* **2005**, *347*, 19–31.
[13] M. A. M. Capozzi, C. Cardellicchio, F. Naso, *Eur. J. Org. Chem.* **2004**, 1855–1863.
[14] M. A. M. Capozzi, C. Cardellicchio, F. Naso, G. Spina, P. Tortorella, *J. Org. Chem.* **2001**, *66*, 5933–5936.
[15] M. A. M. Capozzi, C. Cardellicchio, G. Fracchiolla, F. Naso, P. Tortorella, *J. Am. Chem. Soc.* **1999**, *121*, 4708–4709.
[16] M. A. M. Capozzi, C. Cardellicchio, F. Naso, P. Tortorella, *J. Org. Chem.* **2000**, *65*, 2843–2846.
[17] M. A. M. Capozzi, C. Cardellicchio, F. Naso, V. Rosito, *J. Org. Chem.* **2002**, *67*, 7289–7294.
[18] C. Cardellicchio, O. Hassan Omar, F. Naso, M. A. M. Capozzi, F. Capitelli, V. Bertolasi, *Tetrahedron: Asymmetry* **2006**, *17*, 223–229.
[19] F. Naso, C. Cardellicchio, F. Affortunato, M. A. M. Capozzi, *Tetrahedron: Asymmetry* **2006**, *17*, 3226–3229.
[20] F. Naso, M. A. M. Capozzi, A. Bottoni, M. Calvaresi, V. Bertolasi, F. Capitelli, C. Cardellicchio, *Chem. Eur. J.* **2009**, *15*, 13417–13426.
[21] M. A. M. Capozzi, C. Centrone, G. Fracchiolla, F. Naso, C. Cardellicchio, *Eur. J. Org. Chem.* **2011**, 4327–4334.
[22] K. Okano, *Tetrahedron* **2011**, *67*, 2483–2512.
[23] K. Yamamoto, H. Ando, T. Shuetake, H. Chikamatsu, *J. Chem. Soc. Chem. Commun.* **1989**, 754–755.
[24] M. I. Donnoli, S. Superchi, C. Rosini, *J. Org. Chem.* **1998**, *63*, 9392–9395.
[25] M. Seto, N. Miyamoto, K. Aikawa, Y. Aramaki, N. Kanzai, Y. Iizawa, M. Baba, M. Shiraishi, *Bioorg. Med. Chem.* **2005**, *13*, 363–386.
[26] B. Jiang, X.-L. Zhao, J.-J. Dong, W.-J. Wang, *Eur. J. Org. Chem.* **2009**, 987–991.
[27] M. Nishio, *Phys. Chem. Chem. Phys.* **2011**, *13*, 13873–13900; M. Nishio, Y. Umezawa, K. Honda, S. Tsuboyama, H. Suezawa, *CrystEngComm* **2009**, *11*, 1757–1788; M. Nishio, *CrystEngComm* **2004**, *6*, 130–158; C. Cardellicchio, M. A. M. Capozzi, A. Alvarez-Larena, J. F. Piniella, F. Capitelli, *CrystEngComm* **2012**, *14*, 3972–3981.
[28] M. Nishio, *Tetrahedron* **2005**, *61*, 6923–6950.
[29] N. G. Payne, M. E. Peach, *Sulfur Lett.* **1986**, *4*, 217–221.
[30] D. B. Denney, D. Z. Denney, L. T. Liu, *Phosphorus Sulfur* **1982**, *13*, 1–7.
[31] M. Kersten, E. Wenschuh, *Phosphorus Sulfur* **1993**, *80*, 81–84.
[32] M. E. Peach, A. M. Ritcey, *J. Fluorine Chem.* **1982**, *21*, 401–406.
[33] G. Pescitelli, S. Di Pietro, C. Cardellicchio, M. A. M. Capozzi, L. Di Bari, *J. Org. Chem.* **2010**, *75*, 1143–1154.
[34] H. J. Schneider, *Angew. Chem.* **2009**, *121*, 3982–4036; *Angew. Chem. Int. Ed.* **2009**, *48*, 3924–3977.

[35] S. E. Wheeler, *J. Am. Chem. Soc.* **2011**, *133*, 10262 – 10274; I. Y. Bagryanskaya, Y. V. Gatilov, A. M. Maksimov, V. E. Platonov, A. V. Zibarev, *J. Fluorine Chem.* **2005**, *126*, 1281 – 1287.
[36] S. Tsuzuki, T. Uchimaru, M. Mikami, *J. Phys. Chem. A* **2006**, *110*, 2027 – 2033.
[37] V. R. Thalladi, H.-C. Weiss, D. Bläser, R. Boese, A. Nangia, G. R. Desiraju, *J. Am. Chem. Soc.* **1998**, *120*, 8702 – 8710.
[38] T. S. Thakur, M. T. Kirchner, D. Bläser, R. Boese, G. R. Desiraju, *CrystEngComm* **2010**, *12*, 2079 – 2085.
[39] Nonius, COLLECT and EVAL. 2002 Nonius BV, Delft, The Netherlands.
[40] Bruker SAINT and SADABS, 2001, Bruker AXS Inc., Madison, Wisconsin, USA.
[41] A. Altomare, M. C. Burla, M. Camalli, G. L. Cascarano, C. Giacovazzo, A. Guagliardi, A. G. Moliterni, G. Polidori, R. Spagna, *J. Appl. Crystallogr.* **1999**, *32*, 115 – 119.
[42] G. M. Sheldrick, *SHELXL-97. Program for the Refinement of Crystal Structures*. University of Göttingen, Germany, **1997**.
[43] Y. Zhao, G. Truhlar, *Acc. Chem. Res.* **2008**, *41*, 157 – 167.
[44] Y. Zhao, G. Truhlar, *J. Phys. Chem. A* **2004**, *108*, 6908 – 6918.
[45] Y. Zhao, G. Truhlar, *J. Phys. Chem. A* **2005**, *109*, 5656 – 5667.
[46] Y. Zhao, O. Tishchenko, G. Truhlar, *J. Phys. Chem. B* **2005**, *109*, 19046 – 19051.
[47] Gaussian 03, Revision A.1., M. J. Frisch, G. W. Trucks, H. B. Schlegel, G. E. Scuseria, M. A. Robb, J. R. Cheeseman, J. A. Montgomery, Jr., T. Vreven, K. N. Kudin, J. C. Burant, J. M. Millam, S. S. Iyengar, J. Tomasi, V. Barone, B. Mennucci, M. Cossi, G. Scalmani, N. Rega, G. A. Petersson, H. Nakatsuji, M. Hada, M. Ehara, K. Toyota, R. Fukuda, J. Hasegawa, M. Ishida, T. Nakajima, Y. Honda, O. Kitao, H. Nakai, M. Klene, X. Li, J. E. Knox, H. P. Hratchian, J. B. Cross, V. Bakken, C. Adamo, J. Jaramillo, R. Gomperts, R. E. Stratmann, O. Yazyev, A. J. Austin, R. Cammi, C. Pomelli, J. W. Ochterski, P. Y. Ayala, K. Morokuma, G. A. Voth, P. Salvador, J. J. Dannenberg, V. G. Zakrzewski, S. Dapprich, A. D. Daniels, M. C. Strain, O. Farkas, D. K. Malick, A. D. Rabuck, K. Raghavachari, J. B. Foresman, J. V. Ortiz, Q. Cui, A. G. Baboul, S. Clifford, J. Cioslowski, B. B. Stefanov, G. Liu, A. Liashenko, P. Piskorz, I. Komaromi, R. L. Martin, D. J. Fox, T. Keith, M. A. Al-Laham, C. Y. Peng, A. Nanayakkara, M. Challacombe, P. M. W. Gill, B. Johnson, W. Chen, M. W. Wong, C. Gonzalez, J. A. Pople, Gaussian, Inc., Wallingford CT, **2004**.
[48] N. Godbout, D. R. Salahub, J. Andzelm, E. Wimmer, *Can. J. Chem.* **1992**, *70*, 560 – 571.

Received: July 10, 2012
Published online on November 23, 2012